

# Sustainable adhesive from waste expanded polystyrene: Performance governed by solvent-substrate interplay

Received: 13 November 2025

Accepted: 26 February 2026

Published online: 03 April 2026

Cite this article as: Jobarani R.A., Alkurdi H. & Deri F. Sustainable adhesive from waste expanded polystyrene: Performance governed by solvent-substrate interplay. *Sci Rep* (2026). <https://doi.org/10.1038/s41598-026-42596-8>

Rama AL Jobarani, Hassan Alkurdi & Fawaz Deri

We are providing an unedited version of this manuscript to give early access to its findings. Before final publication, the manuscript will undergo further editing. Please note there may be errors present which affect the content, and all legal disclaimers apply.

If this paper is publishing under a Transparent Peer Review model then Peer Review reports will publish with the final article.

ARTICLE IN PRESS

---

# Sustainable Adhesive from Waste Expanded Polystyrene: Performance Governed by Solvent-Substrate Interplay.

**Rama AL Jobarani<sup>1\*</sup>, Prof. Mhd. Hassan Alkurdi<sup>2</sup>, Prof. Fawaz Deri<sup>3</sup>.**

*<sup>1</sup> PhD student, Department of Chemistry, Faculty of science, Damascus University, Materials Rheology Laboratory, Damascus, Syria.*

*<sup>2</sup> Professor, Department of Chemistry, Faculty of Sciences, Damascus University.*

*<sup>3</sup> Professor, Engineer, Department of Chemistry, Faculty of science, Damascus University, Rheology of plastics materials.*

## **Authors:**

**Rama Al-Joubrani, Fawaz Deri, and Mhd. Hassan Alkurdi.**

## **Affiliations:**

**Department of Chemistry, Damascus University, Damascus, Syria.**

## **Contact Information**

**Corresponding author:** Rama Al Jobarani (email: [ram996jo@gmail.com](mailto:ram996jo@gmail.com).)

## **Abstract**

This study presents a sustainable approach for converting post-consumer Expanded Polystyrene (EPS) into a high-performance adhesive. EPS was dissolved in various organic solvents and modified with PMMA, and the resulting formulations were evaluated chemically, Rheologically, and mechanically. Solubility trends correlated with Hansen Solubility Parameters, with toluene showing the highest dissolution efficiency (RED = 0.65). Rheological analysis revealed near-Newtonian to mildly shear-thinning behavior (STI = 0.018–0.203), indicating viscosity stability suitable for application. Mechanical testing demonstrated strong substrate-dependent performance: xylene-based adhesives achieved high bonding strength on non-polar leather ( $\approx 778$  KPa), while MEK-based formulations exhibited superior adhesion to wood ( $\approx 755$  KPa) due to enhanced hydrogen bonding. Incorporation of PMMA further reinforced the adhesive network, yielding the highest tensile strength ( $\approx 1969$  KPa). All formulations bonded effectively to polyurethane and showed robust qualitative adhesion to ceramic. These findings validate the feasibility of upcycling EPS waste into a versatile, high-strength adhesive, offering a practical and environmentally beneficial solution for plastic waste management.

---

## 1. Introduction

Expanded polystyrene (EPS), commercially known as thermocol, is a lightweight, rigid polymer extensively used in packaging, insulation, and disposable consumer products. Global production exceeds 15 million metric tons annually; however, end-of-life management remains problematic due to inadequate recycling infrastructure and limited reuse pathways. In the United States alone, over 2.3 million tons of EPS waste are landfilled yearly, with recycling rates below 2% [1,2].

A key environmental challenge posed by EPS is its extremely low bulk density, which leads to disproportionate spatial occupation in waste systems. Experimental measurement of EPS samples in this study revealed that one cubic meter weighs only 1440 grams, corresponding to a bulk density of 1.44 kg/m<sup>3</sup>. This volumetric inefficiency means that minimal mass occupies substantial landfill volume, complicating logistics related to collection, transport, and disposal. Moreover, the low mass and high surface area of EPS make it prone to wind dispersal, resulting in widespread littering in terrestrial and aquatic environments.

Among the most concerning consequences of this dispersal is the accidental ingestion of EPS by grazing livestock such as sheep and goats. Field observations confirm that animals can mistake EPS fragments for forage, leading to gastrointestinal blockages, impaired digestion, and in severe cases, death. Figure 1 illustrates this risk, showing sheep feeding near EPS-containing materials in an agricultural setting. Recent physiological studies substantiate these observations: Chang et al. (2024) demonstrated that polystyrene exposure in lambs induces gastrointestinal injury, inflammation, and reduced growth and meat quality [3]. Furthermore, Aardema et al. (2024) emphasized that farm animals constitute a critical link between environmental microplastic pollution and human health, highlighting broader implications for food safety and agricultural productivity [4].

In response to these environmental and agricultural concerns, this study aims to develop and evaluate a sustainable adhesive system derived from post-consumer EPS. By systematically investigating its chemical, rheological, and mechanical properties across multiple substrates, we seek to demonstrate the practical potential of EPS reuse while mitigating its ecological footprint.

Conventional disposal methods such as landfilling and incineration are constrained by spatial inefficiency and environmental impact. Dissolution-based recycling has thus emerged as a promising alternative, offering an energy-efficient and scalable route to polystyrene recovery. This approach involves solubilizing EPS in organic solvents to yield polymer gels or solutions that can be repurposed into adhesives, coatings, or composite materials [5].

Previous research supports the feasibility of this strategy. García et al. (2009) examined polystyrene solubility and stability in various solvents, underscoring its potential for adhesive applications [6]. Selukar (2014) and Kaushal et al. (2018) explored EPS-derived adhesives for construction materials [7,8], while De Paula et al. (2018) investigated its conversion into carbonaceous composites [9]. Notably, Uttaravalli et al. (2021) conducted a comprehensive study on EPS-based adhesives using six solvents—MEK, THF, n-butyl acetate, m-xylene, gasoline, and carbon tetrachloride—and reported that MEK-based formulations exhibited shear strength comparable to commercial adhesives like Fevicol, with successful bonding to wood, paper, and ceramic substrates [10].



**Figure 1. Sheep feeding near EPS-containing materials in a rural setting. The image illustrates the potential risk of accidental ingestion of expanded polystyrene (EPS) by grazing livestock, which may lead to digestive complications and broader implications for animal welfare and food safety.**

Building on this foundation, the present work introduces a novel adhesive system derived entirely from post-consumer EPS, with a focus on mechanical performance across diverse substrates including wood, leather, ceramic, and polyurethane—the latter specifically relevant to footwear soles.

This study distinguishes itself by integrating rheological analysis, tensile testing, and substrate-specific adhesion mechanisms, along with a comparative evaluation of solvent compatibility and additive effects. The inclusion of polyurethane extends the practical applicability of the adhesive, particularly in contexts such as shoe manufacturing and repair.

## **2. Materials.**

### **2.1. Expanded Polystyrene (EPS) Waste and Bulk Density Determination.**

Post-consumer Expanded Polystyrene (EPS) waste was collected as the primary raw material. To accurately determine its characteristic low bulk density—a key factor in its environmental impact—a practical approach was employed. Multiple EPS packages were assembled to form a large composite structure with dimensions closely approximating 1 m<sup>3</sup> (1 m × 1 m × 1 m). The total mass of this assembly was measured using a calibrated scale and found to be 1440 g. The bulk density was subsequently calculated as:

$$\rho = \frac{m}{V} = \frac{1440\text{g}}{1\text{m}^3} = 1.440\text{kg/m}^3$$

This method effectively captures the real-world volumetric inefficiency of EPS waste. A photograph of the assembled sample is provided in Figure 2 to illustrate the sampling geometry and scale.

## 2.2. Solvents.

The following organic solvents were used as received without further purification:

- **Methyl Ethyl Ketone (MEK)**, high purity (Puro), supplied by Carlo Erba (Code No. 354253).
- **Benzene**, 99.8% purity, supplied by Panreac (Code: 161192.1612).
- **Toluene**, PRS grade, supplied by Panreac (Code: 141745.1612).
- **Xylene**, supplied by Panreac, with a purity of 99.5% (by GC).

## 2.3. Additive.

Poly(methyl methacrylate) (PMMA) was supplied by Kumho Petrochemical Co., Ltd. (South Korea) and used as a reinforcing polymer additive.



---

**Figure 2. Photograph of the assembled EPS sample used for bulk density determination (approximate volume: 1 m<sup>3</sup>; measured mass: 1440 g).**

### **3. Methodology.**

#### **3.1 Sample Preparation.**

Samples of recycled Expanded Polystyrene (EPS) were prepared by collecting EPS waste, shredding it into small pieces, and subsequently dissolving it in various organic solvents, including benzene, toluene, xylene, and methyl ethyl ketone (MEK). All basic adhesive formulations maintained a constant polymer-to-solvent mass ratio of 30:70, where the polymer component consisted solely of EPS.

Based on preliminary positive results in bonding applications on wood, two additional adhesive formulations were developed using methyl ethyl ketone as the primary solvent:

- The first formulation (EPS(M+T)) consisted of 30% EPS dissolved in a blended solvent system of 35% Methyl Ethyl Ketone and 35% Toluene.
- The second formulation (EPS(M+PMMA)) was modified by replacing part of the polymer content. It consisted of 30% EPS and 5% Poly (methyl methacrylate) (PMMA) as the polymer phase, dissolved in 65% Methyl Ethyl Ketone.

All mixtures were stirred using a mechanical stirrer at 100 RPM for 4 hours at ambient temperature until complete dissolution was achieved. Table 1 details the complete compositions and nomenclature of all prepared samples.

#### **3.2 Chemical Properties Testing.**

##### **3.2.1 Solubility Determination.**

The solubility of EPS in the various solvents was determined gravimetrically, considering the minimum amount of solvent required to dissolve a pre-weighed sample of EPS (2g). The solubility was calculated using the following equation [6]:

$$\text{solubility} \left( \frac{\text{g}}{\text{ml}} \right) = \frac{\text{EPS weight (g)}}{\text{Solvent volume (ml)}} \quad (1)$$

The experiment was repeated three times. The solubility values were consistent across all replicates, indicating good reproducibility. All measurements exhibited a coefficient of variation (CV) of less than 5.7%, confirming the accuracy and reliability of the obtained results.

---

**Table 1: Composition and Nomenclature of Prepared EPS Adhesive Formulations.**

dissolved substance	solvent	Additive	The symbol
Expanded Polystyrene (EPS)	Benzene		EPS(B)
	Toluene		EPS(T)
	Xylene		EPS(X)
	Methyl ethyl ketone		EPS(MEK)
	Toluene + Methyl ethyl ketone		EPS(T+MEK)
	Methyl ethyl ketone	PMMA	EPS (M+ PMMA)

### 3.2.2 Evaporation Rate.

The evaporation rate of the prepared adhesive samples was measured using a precise balance. The samples were weighed to four decimal places and their mass was measured again after one hour. The objective of this test was to determine the evaporation rate of the solvents in the EPS adhesives, to aid in the subsequent interpretation of adhesive strength. The evaporation rate was calculated as the percentage loss of mass (LM) using the following equation <sup>[11]</sup>:

$$LM = \frac{m_i - m_f}{m_i} \times 100 \quad (2)$$

Where  $m_i$  and  $m_f$  are the initial and final mass of the sample before and after solvent evaporation, respectively. All measurements showed high repeatability with a coefficient of variation (CV) of less than 0.11%, confirming the precision and reliability of the data.

### 3.3 Rheological Properties Testing.

The rheological properties of the samples were tested using a Fungilab Expert R Viscometer. To ensure accurate measurements, the spindle and rotational speed range were selected for each formulation to maintain the torque percentage within the valid instrument range of 20% to 90%. Accordingly, spindle R5 was used with a rotational speed range of 5, 7.5, 10, 12, 15, 20, 25, and 30 RPM for the EPS(B) sample. For the remaining formulations, spindle R4 was employed with a speed range of 35, 40, 50, 60, 70, 80, and 90 RPM.

#### 3.3.1 Viscosity Measurement and Rheological Analysis.

The apparent viscosity of the prepared adhesive formulations was measured directly in centipoise (cP) using a Fungilab Expert R

Viscometer. To enable comprehensive rheological characterization, the fundamental parameters of shear rate ( $\dot{\gamma}$ ) and shear stress ( $\tau$ ) were derived from the raw viscometer data using the following conversion equations:

$$\dot{\gamma} = K_1 \times \text{RPM} \quad (3)$$

$$\tau = K_2 \times \text{Torque\%} \quad (4)$$

Where  $K_1$  and  $K_2$  are factors dependent on the spindle number [12].

$K_1 = 0.21, 0.17$  ( $\text{sec}^{-1}$ ) for spindles R4 and R5, respectively.

$K_2 = 0.430, 0.860$  ( $\text{dyne/cm}^2$ ) for spindles R4 and R5, respectively.

### **3.3.2 Shear-Thinning Index (STI) Test.**

The Shear-Thinning Index (STI), which serves as a tool for estimating the degree of non-Newtonian behavior, was determined using a method analogous to the ASTM E3070 standard. (**ASTM E3070-18 Standard Test Method**) [13]. This index is calculated from the difference in viscosity measured at the lowest and highest shear rates. An STI value of 0 indicates perfect Newtonian behavior, while an  $\text{STI} > 0$  indicates shear-thinning (pseudoplastic) behavior. This index reflects the extent of polymer structural breakdown upon the application of shear and is also known as the Pseudoplastic Index. It was calculated as:

$$\text{STI} = \frac{\eta_{\text{low shear}} - \eta_{\text{high shear}}}{\eta_{\text{low shear}}} \quad (5)$$

### **3.4 Mechanical Properties Testing.**

The adhesive strength (bonding strength) was evaluated via a tensile test using an Instron Universal Testing Machine. The adhesive was applied to substrates including leather, polyurethane foam, wood, and ceramic, with bonding dimensions of 25 mm  $\times$  25 mm and a thickness of 0.5 mm. For each substrate type, 14 samples were prepared, and each sample was tested in triplicate to ensure statistical reliability. After application, a constant load was applied to each bonded specimen for 48 hours to maintain uniform pressure and allow complete curing prior to testing. All tests were conducted at a controlled temperature of 22.8 °C and 50% relative humidity.



**Figure 3. Labeled experimental samples prepared for tensile adhesion testing.**

## **4. Results and Discussion.**

### **4.1 Solubility Determination.**

The solubility of EPS in various solvents was evaluated both experimentally and theoretically using the Hansen Solubility Parameters (HSP) framework. According to this model, the relative energy difference (RED), defined as  $RED = R_a/R_0$ , predicts solubility likelihood. An RED value less than 1 indicates a high probability of dissolution, while values increasingly greater than 1 suggest lower solubility [14]. The distance  $R_a$  between the solvent and polymer in Hansen space was calculated using the equation:

$$(R_a) = \sqrt{4\Delta D^2 + \Delta P^2 + \Delta H^2}$$

where  $\Delta\delta D$ ,  $\Delta\delta P$ , and  $\Delta\delta H$  are the differences in the dispersion, polar, and hydrogen-bonding solubility parameters, respectively, between the solvent and EPS [15], and  $R_0$  is the radius of the solubility sphere of EPS ( $12.7 \text{ MPa}^{1/2}$ ) [16].

As presented in Table 2, the experimental solubility results show a strong correlation with the calculated RED values. Toluene, with the lowest RED value (0.65), exhibited the highest solubility (0.605 g/ml), whereas Methyl Ethyl Ketone, with the highest RED value (0.84), demonstrated the lowest solubility (0.487 g/ml). This remarkable agreement confirms the predictive power of the HSP model [17]. The superior performance of Toluene is attributed to its optimal combination of a low RED number, favorable molecular compatibility with non-polar EPS, and properties that facilitate rapid diffusion into the polymer's cellular structure, as supported by its high self-diffusion coefficient reported in polystyrene solutions [18]. The intermediate solubility of Xylene (RED = 0.67, Solubility = 0.527 g/ml) and Benzene (RED = 0.67, Solubility = 0.495 g/ml) aligns with this rationale. The subtle performance difference between them can be attributed to their

intrinsic physicochemical properties. Data from the DIPPR database indicates that Benzene possesses a higher volatility and a lower dynamic viscosity compared to Xylene. This likely causes Benzene to evaporate more rapidly during the dissolution process, thereby reducing its practical effectiveness despite its theoretical compatibility being nearly identical to that of Xylene [19]. In contrast, Methyl Ethyl Ketone's higher polarity, reflected in its elevated RED value, along with its distinct solvent properties, fundamentally limit its interaction with the non-polar EPS matrix.

**Table 2. Experimental Solubility of EPS and Correlation with Hansen Solubility Parameters.**

Solvent	EPS solubility (g/ml)	$\delta\text{MPa}^{1/2}$			Vaper Pressure at 25°C (KPa)	$R_a$ (MPa <sub>0.5</sub> )	RED = $R_a/R_0$
		$\delta_D$	$\delta_P$	$\delta_H$			
EPS	-	21.3	5.8	4.3	-	-	-
Toluene	0.605 ± 0.053	18	1.4	2	3.87	8.26	0.650
xylene	0.527 ± 0.027	17.8	1	4.1	1.17	8.49	0.668
Benzene	0.495 ± 0.001	18.4	0	2	12.58	8.52	0.670
Methyl ethyl Ketone	0.487 ± 0.001	16	6.3	5.1	10.37	10.64	0.837

\***Note:** The Hansen parameters for EPS and solvent are from reference data (Burke, J. (1984)) [20], (Lide, D. R. (1991)) [21]. \*

#### 4.2 Evaporation rate.

As delineated in Table 3, the evaporation rates of the prepared adhesive formulations exhibit a clear correlation with the intrinsic volatility of their constituent solvents. The EPS(B) sample demonstrated the highest evaporation rate (35.19%), which is consistent with the high volatility inherent to benzene. This was followed by EPS(X), EPS(T), and the blend EPS(M+T). A significant decrease in evaporation rate was observed for the MEK-based formulations, with EPS(MEK) and EPS(M+PMMA) showing the lowest values (28.45% and 24.87%, respectively). This can be attributed to the lower volatility of MEK and the further vapor-pressure depression caused by the dissolution of the PMMA polymer additive.

**Table 3. Evaporation rates of the prepared EPS adhesive formulations.**

Samples	Evaporation rate (%)
EPS(T)	<b>34.13</b> ± 1.45
EPS(X)	<b>34.31</b> ± 2.52
EPS(B)	<b>35.19</b> ± 0.40
EPS(MEK)	<b>28.45</b> ± 1.99

EPS (M+T)	<b>33.74</b> ± 2.68
EPS (M+ PMMA)	<b>24.87</b> ± 1.88

An important experimental observation for the MEK-based adhesives was the rapid formation of a superficial skin or layer at the air-adhesive interface immediately after application. This phenomenon, where solvent evaporation leads to a concentrated polymer layer that can hinder further solvent loss from the underlying bulk, is a recognized characteristic in polymer solutions and adhesive science [11]. This skin formation effectively reduces the overall evaporation rate and can influence the adhesive's open time and bonding characteristics.

### 4.3 Rheological Properties.

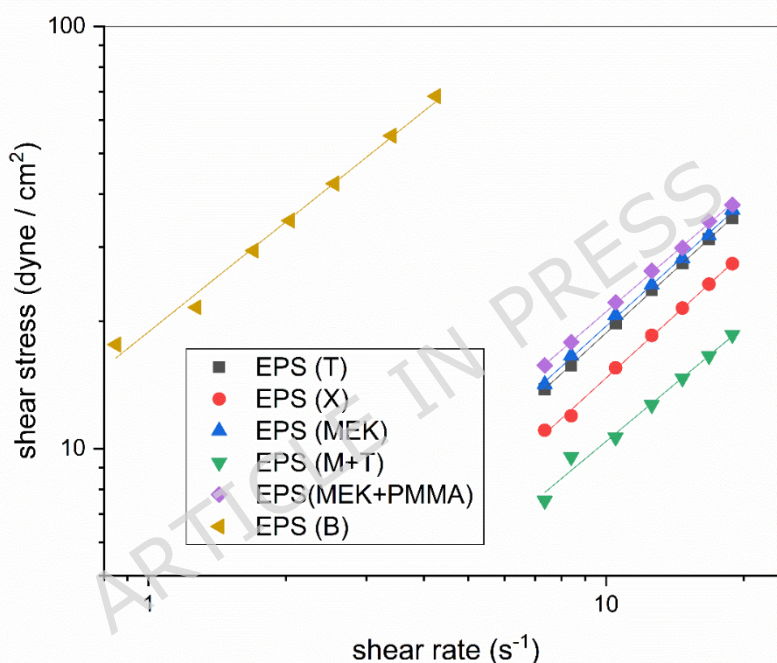
The rheological behavior of the prepared adhesive formulations was analyzed to assess their flow characteristics, which are critical for application performance. Figure 4 illustrates the relationship between shear stress and shear rate for all samples, fitted using the Power-Law model ( $\tau = K\dot{\gamma}^n$ ). As summarized in Table 4, the consistency index  $K$  showed significant variation among samples, with EPS(B) exhibiting the highest value (18.87 dyne·s<sup>n</sup>/cm<sup>2</sup>), indicating greater resistance to flow, while other formulations showed substantially lower values ranging from 1.29 to 2.46 dyne·s<sup>n</sup>/cm<sup>2</sup>.

The flow behavior indices ( $n$ ) ranged between 0.868 and 0.989, indicating near-Newtonian to weakly shear-thinning behavior. The high  $n$  values for EPS(T) and EPS(X) (0.989 and 0.986, respectively) confirm their approximately Newtonian flow, consistent with their excellent solvent quality. This near-Newtonian behavior in well-compatible polymer-solvent systems has been previously reported by (Serin et al., 2016). for polystyrene solutions [22].

The Shear-Thinning Index (STI) provides further insight into the non-Newtonian character. The STI values, calculated according to Equation (5), ranged from 0.018 for EPS(X) to 0.203 for EPS(B). The low STI values for EPS(T) and EPS(X) confirm their nearly Newtonian flow, attributed to their high compatibility with EPS, as indicated by their low RED values, which promotes effective chain dissolution and minimal structural resistance to shear. In contrast, EPS(B) exhibited the highest STI value, signifying the most pronounced shear-thinning behavior [23]. This can be linked to its higher consistency index ( $K$ ) and the use of a different spindle geometry, which may have induced localized shear deformations. The moderate STI values for MEK-based systems (EPS(MEK) and EPS(M+PMMA)) suggest that despite the solvent's higher polarity, these formulations still display measurable non-Newtonian character, potentially due to dipole-dipole interactions promoting temporary clustering.

**Table 4. Rheological parameters of EPS adhesive formulations obtained from Power-Law model fitting and Shear-Thinning Index (STI).**

Samples	EPS (T)	EPS (X)	EPS (B)	EPS (MEK)	EPS (M+T)	EPS (M+PMMA)
<b>n</b>	0.989	0.986	0.868	0.981	0.902	0.931
<b>K (dyne.s<sup>n</sup>/c m<sup>2</sup>)</b>	1.92	1.51	18.87	2.03	1.29	2.46
<b>R<sup>2</sup></b>	0.999	0.997	0.991	0.998	0.987	0.999
<b>STI</b>	0.035	0.018	0.203	0.052	0.027	0.066

**Figure 4. Flow curves of the prepared EPS adhesive formulations.**

The viscosity profiles, depicted in Figure 5, show a slight shear-thinning tendency, particularly for the EPS(MEK) system. The EPS (MEK) and EPS (B) combinations showed a slight downward slope, consistent with their higher STI values. Conversely, EPS(T) and EPS(X) maintained almost constant viscosity across the measured shear rate range, underscoring their Newtonian-like response and excellent solvent quality, which reduces viscosity dependence on shear.

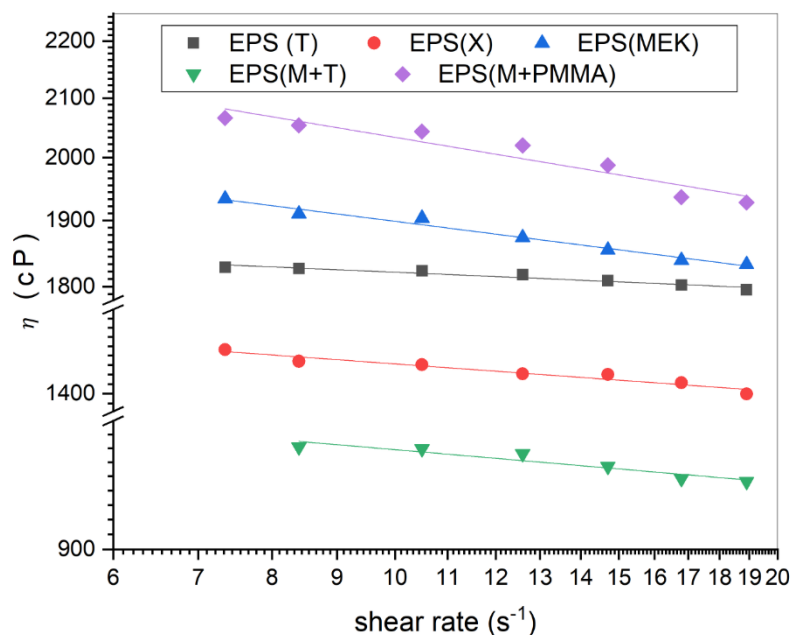


**Figure 5. Apparent viscosity as a function of shear rate for the EPS adhesive formulations.**

From a processing standpoint, these results highlight how solvent selection governs adhesive behavior during application. Systems with nearly constant viscosity (X and T) are ideal for controlling spread and film uniformity, as discussed in rheological studies of adhesive systems [24]. In contrast, formulations with higher  $K$  and moderate shear-thinning (B and MEK) may offer advantages like enhanced wetting under high shear and improved cohesion at rest, a rheological duality crucial for optimizing adhesive performance.

#### 4.4 Mechanical Properties.

##### 4.4.1 Performance on Leather Substrate.

Table 5 and Figure 6 shows that sample EPS(X) recorded the highest maximum stress on belt leather, reaching 778.069 KPa, outperforming EPS(T) (700.39 KPa) and EPS(B) (632.4 KPa). This superiority is explained by the balanced interplay between the adhesive's rheological and chemical properties.

The superior performance of EPS(X) on leather (778.069 KPa) is attributed to a synergistic combination of favorable rheology and chemical compatibility. Its near-Newtonian behavior ( $n = 0.986$ ) ensures uniform application and stable viscosity under shear, preventing premature structural collapse during spreading. Chemically, the low RED value (0.668) indicates high affinity between xylene and the non-polar EPS matrix, promoting efficient dissolution and chain mobility. This, coupled with an optimal evaporation rate (34.31%), facilitates deep penetration

into the leather's micro-porous structure, forming robust mechanical interlocks. In contrast, the pronounced shear-thinning of EPS(B) (STI = 0.203) and its higher volatility likely hinder penetration, resulting in weaker interfacial bonding.

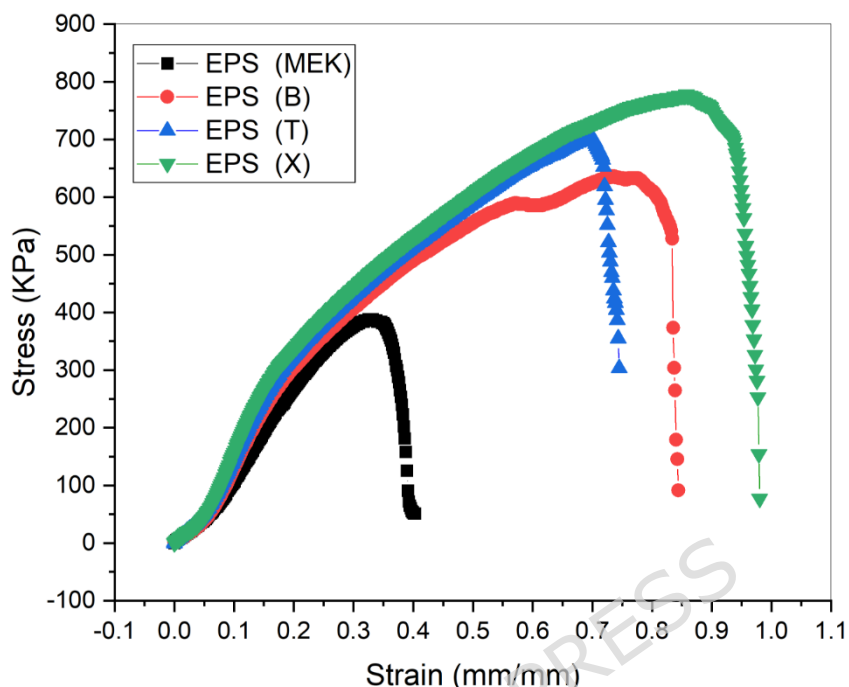


**Figure 6. Tensile stress-strain curves of the prepared EPS adhesive formulations on leather substrate.**

Consequently, EPS(X)'s advantage over toluene and benzene formulations stems from an optimal balance of viscosity, evaporation rate, and chemical compatibility, making it superior on belt leather in terms of adhesive strength and application stability. By contrast, EPS(MEK) exhibited the lowest maximum stress (306.97 KPa), associated with its low evaporation rate (23.45%) and higher RED (0.837), indicating poor compatibility with the base polymer, reduced penetration into the leather, and lower bond strength. This observed trend aligns with the diffusion theory of adhesion, where effective polymer chain interlocking is governed by solvent quality and evaporation kinetics [25,11].

#### **4.4.2 Performance on Wood Substrate and Performance Enhancement with Additives.**

The mechanical performance of EPS-based adhesives on wood varied significantly across formulations (Figure 7, Table 5). EPS(MEK) exhibited the highest tensile strength (754.78 KPa), followed by EPS(B) (707.58 KPa) and EPS(T) (604.72 KPa). In contrast, EPS(X) showed a substantially lower strength (445.49 KPa) and no measurable spontaneous breaking stress. This limited performance is likely due to its rapid evaporation and quasi-

Newtonian behavior ( $n = 0.986$ ,  $STI = 0.018$ ), which favors surface-level coverage over deep penetration into the porous wood matrix, potentially resulting in adhesive or interfacial failure during testing.

The superior adhesion of EPS(MEK) stems not only from its moderate evaporation rate (28.45%) but also from its intrinsic chemical affinity for wood. As a polar aprotic solvent, methyl ethyl ketone (MEK) contains a carbonyl group capable of forming hydrogen bonds with the hydroxyl-rich cellulose in wood. These interactions enhance interfacial adhesion via dipole-dipole and hydrogen-bonding mechanisms, thereby improving mechanical stability and bond strength. This aligns with the diffusion theory of adhesion, which underscores the importance of molecular interactions and solvent-substrate compatibility [25,26,27,28]. Recent reviews further emphasize how solvent polarity and functional group availability modulate hydrogen bonding in wood adhesion [26,29], and studies confirm that ketone-based solvents such as MEK can engage in transient hydrogen bonding with cellulose, influencing both wetting and adhesion [30,31].

Performance was further elevated with the addition of poly (methyl methacrylate) (PMMA) in the EPS(M+PMMA) formulation, which achieved a remarkable tensile strength of (1968.62KPa). Beyond simply reinforcing the polymer matrix, PMMA introduces additional polar carbonyl groups that can form hydrogen bonds with cellulose hydroxyls, strengthening interfacial compatibility and molecular anchoring [26,32,33]. PMMA and its copolymers are known to establish stable hydrogen-bonded networks with cellulose derivatives, affecting both adhesion and viscoelastic behavior at the interphase [29,30]. For instance, Fahrländer et al. (2001) showed that PMMA particles alter the rheology of polystyrene matrices, enhancing structural cohesion and flow characteristics via interfacial interactions and phase morphology [34]. Thus, PMMA acts synergistically as both a mechanical reinforcer and a chemical mediator that promotes interfacial cohesion and rheological stability.

**Table 5: Caption: Mechanical performance of EPS adhesive samples on substrates (maximum stress and displacement data).**

<b>Substrate</b>	<b>Leather</b>			
<b>Samples</b>	<b>STRESS (Max Load) (KPa)</b>	<b>Strain (Max Disploment) (mm/mm)</b>	<b>STRESS (Load Auto Break) (KPa)</b>	<b>Strain (Disploment at Auto Break) (mm/mm)</b>
EPS (T)	700.39	0.694	577.34	0.72
EPS (X)	778.069	0.857	629.34	0.947
EPS (B)	632.4	0.760	527.89	0.833
EPS (MEK)	306.97	0.371	158.14	0.387
<b>Substrate</b>	<b>Polyurethane Foam</b>			
	The sample was cut outside the adhesion area.			

Substrate	Wood			
EPS (T)	604.72	0.0372	1841.21	0.0359
EPS (X)	445.49	0.1255	No value	No value
EPS (B)	707.58	0.0275	1543.97	0.0258
EPS (MEK)	754.78	0.0481	3184.44	0.0471
EPS (M+T)	135.25.0	0.0323	1081.48	0.028
EPS (M+PMMA)	1968.62	0.0295	2010.88	0.0284

Additional benefits of PMMA include improved film integrity, reduced solvent evaporation, and more uniform stress distribution—all critical for durable adhesion [27]. The enhanced performance of EPS(M+PMMA) is therefore attributed to a dual mechanism: (1) mechanical reinforcement of the adhesive matrix and (2) interfacial synergy through hydrogen bonding and polarity matching with cellulose [26,35].

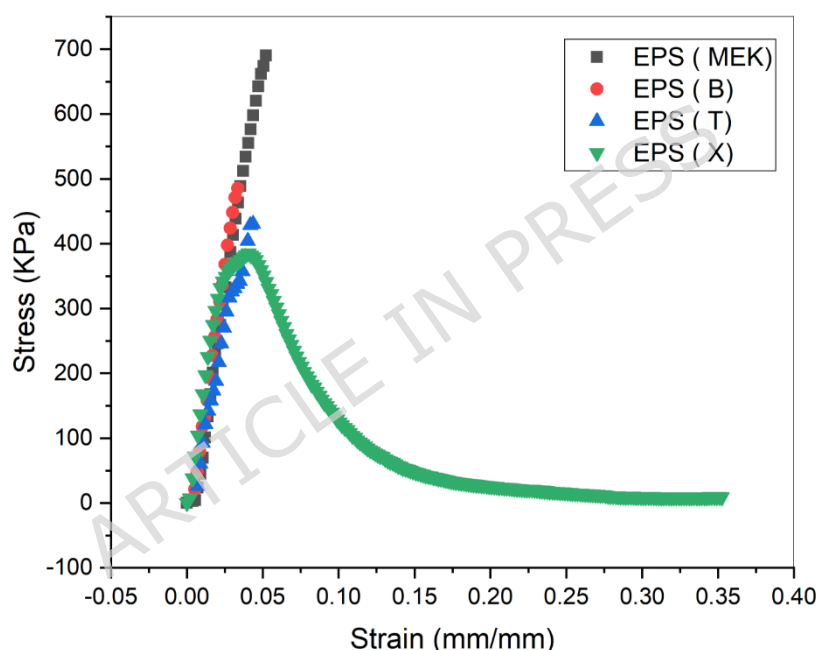


**Figure 7. Tensile stress-strain curves of the prepared EPS adhesive formulations on wood substrate.**

Conversely, the EPS(M+T) formulation displayed markedly lower strength (135.25 KPa), likely due to competitive solvent interactions that disrupt optimal hydrogen bonding and reduce permeability. These results underscore the critical influence of solvent-substrate compatibility and molecular-level interactions on adhesive performance.

#### **4.4.3 Performance on Polyurethane Substrate.**

Tensile testing on polyurethane foam—representative of commercial shoe sole material—revealed a consistent and significant failure mode across all

adhesive formulations. In every case, rupture occurred cohesively within the polyurethane substrate itself, rather than at the adhesive-substrate interface or within the adhesive layer. This cohesive substrate failure provides definitive evidence that the adhesive strength of every EPS-based formulation surpassed the intrinsic cohesive strength of the polyurethane material. Such a failure mode represents an ideal bonding outcome in practical terms, particularly for footwear repair and manufacturing, where adhesion must reliably exceed the substrate's own integrity.

While this failure mode precluded the extraction of precise numerical adhesive strength values, the consistent observation of substrate failure unequivocally validates the exceptional bonding capability of the developed adhesives for shoe-sole applications. This interpretation aligns with established adhesive testing standards (e.g., ASTM D4541/D7234), where substrate failure is recognized as an indicator of optimal adhesive performance [29].

#### **4.4.4 Performance on Ceramic Substrate.**

The intrinsically brittle nature of ceramics presented significant challenges for conventional tensile testing. As shown in Figure 8, ceramic specimens consistently underwent premature fracture at the gripping points under minimal applied stress, precluding the collection of reliable quantitative tensile data. This behavior aligns with the well-documented low fracture toughness of ceramic materials, which renders them susceptible to catastrophic failure under tensile loading.



**Figure 8. Fracture of ceramic specimens during tensile testing due to brittle failure at the gripping jaws.**

Despite these limitations, the adhesive's performance on ceramic substrates was effectively assessed through qualitative pull-off tests. Following application and curing, the bonded ceramic interface demonstrated remarkable mechanical integrity, resisting manual separation attempts (Figure 9). This robust adhesion, even under qualitative hand-driven loading [10], indicates strong interfacial compatibility. The observed performance is likely attributable to effective

adhesive wetting and micro-mechanical interlocking with the textured ceramic surface, compensating for the lack of quantitative tensile metrics.



**Figure 9. Adhesive application on ceramic substrate showing intact bonding interface after manual tensile loading.**

#### 4.5 Sustainability Considerations and Future Directions.

While the present study validates the technical feasibility of recycling EPS waste into high-performance adhesives, broader sustainability considerations must be acknowledged. The valorization of post-consumer EPS contributes to reducing plastic waste volume and landfill burden, thereby supporting circular-economy principles [35]. However, the solvents employed—benzene, toluene, xylene, and MEK—are associated with environmental and health risks. Benzene is classified as a human carcinogen, while toluene and xylene are known to cause neurological effects upon prolonged exposure. MEK, although less toxic, can still induce irritation and requires controlled handling [36,37]. Thus, strict safety protocols and the exploration of greener, bio-based alternatives are essential to align adhesive development with sustainability goals [38].

Although the adhesive developed in this study is not biobased in its chemical origin, its environmental relevance aligns with the broader principles of biobased and low-impact materials. Recent literature highlights those sustainable adhesive technologies are not limited to biomass-derived polymers but also include systems that reduce fossil-resource consumption and overall carbon footprint through recycling and circular-economy strategies. Upcycling post-consumer EPS into a functional adhesive directly offsets the production of virgin polystyrene and reduces landfill accumulation, thereby lowering greenhouse-gas emissions associated with polymer manufacturing. This

perspective is consistent with modern sustainability frameworks, which classify waste-derived materials as contributors to carbon reduction and resource efficiency, similar to the environmental benefits reported for biobased wood adhesives in recent studies such as Calvez et al. (2024), Calovi et al. (2024), and Ghaffar & Fan (2024, Coatings) [39,40,41]. Therefore, the recycled EPS adhesive developed here provides an environmentally favorable alternative to conventional solvent-borne systems, even if not biobased in origin.

In addition, although the mechanical data presented here provide strong evidence of substrate-specific performance, direct characterization of the adhesive bonding mechanism remains limited. Future studies should employ contact angle measurements to quantify wetting behavior and FTIR spectroscopy to probe hydrogen bonding and interfacial chemistry, thereby offering more definitive mechanistic insights [25]. Furthermore, comparative evaluation between adhesives derived from recycled EPS and those prepared from virgin PS would clarify the performance trade-offs and reinforce the sustainability justification of recycling [25,38].

By integrating these considerations, subsequent research can strengthen both the environmental relevance and the scientific rigor of EPS-based adhesives, ensuring that their application not only addresses waste-management challenges but also advances sustainable materials science.

## **5. Conclusions.**

Collectively, this work establishes a sustainable pathway for valorizing EPS waste into high-performance adhesives, underpinned by a solvent-substrate design principle. By strategically matching solvent polarity with substrate chemistry—non-polar aromatics for leather, polar ketones for wood—we demonstrate that tailored formulations can compete with conventional adhesives. This approach not only mitigates plastic pollution but also offers a versatile material solution for industries ranging from footwear to construction, highlighting the potential of waste-centric circular economy models.

## **Conflict of Interest.**

The authors declare no conflict of interest.

## **Funding.**

No funding was received for conducting this study.

## **Ethics Approval.**

---

---

Not applicable.

### **Data Availability.**

All data generated or analyzed during this study are included in this published article.

### **Author Contributions Statement.**

R.A.J. designed the study, conducted the experiments, analyzed the data, and wrote the main manuscript text.

F.D. and M.H.A. supervised the research, validated the results, and critically reviewed and edited the manuscript.

All authors reviewed and approved the final version of the manuscript.

## **6. References.**

- [1] Prabhakar, R. P., Sanket, S. S., Rauphunnisa, F. I., & Rahul, B. P. (2016). Impacts of thermocol waste on marine life: A review. *Int. Mult. Res. J*, 3, 60-68.
- [2] Kim, S. S., & Kim, S. (2004). Pyrolysis characteristics of polystyrene and polypropylene in a stirred batch reactor. *Chemical Engineering Journal*, 98(1-2), 53-60.
- [3] Chang, X., Li, Y., Han, Y., Fang, Y., Xiang, H., Zhao, Z., ... & Zhong, R. (2024). Polystyrene exposure induces lamb gastrointestinal injury, digestive disorders and inflammation, decreasing daily gain, and meat quality. *Ecotoxicology and Environmental Safety*, 277, 116389.
- [4] Aardema, H., Vethaak, A. D., Kamstra, J. H., & Legler, J. (2024). Farm animals as a critical link between environmental and human health impacts of micro-and nanoplastics. *Microplastics and Nanoplastics*, 4(1), 5.
- [5] García, M. T., Duque, G., Gracia, I., de Lucas, A., & Rodríguez, J. F. (2009). Recycling extruded polystyrene by dissolution with suitable solvents. *Journal of material cycles and waste management*, 11(1), 2-5.
- [6] García, M. T., Gracia, I., Duque, G., De Lucas, A., & Rodríguez, J. F. (2009). Study of the solubility and stability of polystyrene wastes in a dissolution recycling process. *Waste management*, 29(6), 1814-1818.
- [7] Selukar, N. B., Lande, C. V., & Ingole, C. G. (2014). Waste thermocol to adhesive for better environment. *Int J Innov Res Adv Eng*, 1(6), 98-100.
-

- 
- [8] Kaushal, H., Gautam, S., Manjusha, D., & Faisal, S. (2018). Adhesive from petrol and thermocol. *International Journal of Trend in Scientific Research and Development*, 2(3), 2491-2493.
- [9] De Paula, F. G., de Castro, M. C., Ortega, P. F., Blanco, C., Lavall, R. L., & Santamaría, R. (2018). High value activated carbons from waste polystyrene foams. *Microporous and mesoporous materials*, 267, 181-184.
- [10] Uttaravalli, A. N., Dinda, S., Gidla, B. R., Kasturi, G., Kasala, P., & Penta, G. (2021). Studies on development of adhesive material from post-consumer (waste) expanded polystyrene: a two-edged sword approach. *Process Safety and Environmental Protection*, 145, 312-320.
- [11] Bail, M., Malacarne-Zanon, J., Silva, S. M. A., Anauate-Netto, A., Nascimento, F. D., Amore, R., ... & Carrilho, M. R. (2012). Effect of air-drying on the solvent evaporation, degree of conversion and water sorption/solubility of dental adhesive models. *Journal of Materials Science: Materials in Medicine*, 23(3), 629-638.
- [12] Viscometer, M. L. B. (2006). More Solutions to Sticky Problems: A Guide to Getting More from Your Brookfield Viscometer. Brookfield Engineering Labs. Inc.
- [13] ASTM E3070-18 Standard Test Method for Shear Thinning Index of Non-Newtonian Liquids Using a Rotational Viscometer; ASTM International: West Conshohocken, PA, USA, 2018.
- [14] Hansen, C. M. (2004). 50 Years with solubility parameters—past and future. *Progress in organic coatings*, 51(1), 77-84.
- [15] Hansen, C. M. (2004). Aspects of solubility, surfaces and diffusion in polymers. *Progress in organic coatings*, 51(1), 55-66.
- [16] Hildebrand, J.H., 1924. Solubility. Ph.D. Thesis. University of California. Hoernschemeyer, D., 1974. The influence of solvent type on the viscosity of concentrated polymer solutions. *Journal of Applied Polymer Science* 18, 61-75.
- [17] Venkatram, S., Kim, C., Chandrasekaran, A., & Ramprasad, R. (2019). Critical assessment of the Hildebrand and Hansen solubility parameters for polymers. *Journal of chemical information and modeling*, 59(10), 4188-4194.
- [18] Meistermann, L., Duval, M., & Tinland, B. (1997). Self-diffusion coefficient studies in polystyrene/polystyrene/toluene solutions: Dynamic light scattering and fluorescence recovery after photobleaching experiments. *Polymer bulletin*, 39(1), 101-108.
- [19] Rogers, T. N., & Zei, D. A. AIChE/DIPPR® Project ESP Environmental and Safety Properties Policy and Procedures Guidelines.
-

- 
- [20] Burke, J. (1984). Solubility parameters: theory and application.
- [21] Lide, D. R., Baysinger, G., Berger, L. I., Goldberg, R. N., Kehiaian, H. V., Kuchitsu, K., ... & Zwillinger, D. (1991). CRC Handbook of Chemistry and Physics Editor-in-Chief.
- [22] Serin, S. C., Dake, G. R., & Gates, D. P. (2016). Addition-Isomerization Polymerization of Chiral Phosphaalkenes: Observation of Styrene-Phosphaalkene Linkages in a Random Copolymer. *Macromolecules*, *49*(11), 4067-4075.
- [23] Mumbach, G. D., Bolzan, A., & Machado, R. A. F. (2020). A closed-loop process design for recycling expanded polystyrene waste by dissolution and polymerization. *Polymer*, *209*, 122940.
- [24] Larson, R. G., & Desai, P. S. (2015). Modeling the rheology of polymer melts and solutions. *Annual Review of Fluid Mechanics*, *47*(1), 47-65.
- [25] Voiutskii, S. S. (1963). *Autohesion and adhesion of high polymers* (Vol. 4). Wiley.
- [26] Zhang, T., Hu, Y., Dong, Y., Jiang, S., & Han, X. (2025). The Influence of Hydrogen Bonding in Wood and Its Modification Methods: A Review. *Polymers*, *17*(15), 2064.
- [27] Ebnesajjad, S. (2010). *Handbook of adhesives and surface preparation: technology, applications and manufacturing*. William Andrew.
- [28] Kinloch, A. J. (2012). *Adhesion and adhesives: science and technology*. Springer Science & Business Media.
- [29] Standard, A. S. T. M. (2009). Standard test method for pull-off strength of coatings using portable adhesion testers (ASTM D4541). *ASTM International: West Conshohocken, PA*.
- [30] Wohler, M., Benselfelt, T., Wågberg, L., Furó, I., Berglund, L. A., & Wohler, J. (2022). Cellulose and the role of hydrogen bonds: not in charge of everything. *Cellulose*, *29*(1), 1-23.
- [31] Pizzi, A. (2006). \*Adhesion mechanisms in bonding wood\*. In *Handbook of Adhesive Technology* (pp. 547-570). CRC Press.
- [32] Bhat, D. K., & Kumar, M. S. (2006). Biodegradability of PMMA blends with some cellulose derivatives. *Journal of Polymers and the Environment*, *14*(4), 385-392.
- [33] Cavallo, V., Roggero, A., Fina, A., Gerard, J. F., & Pruvost, S. (2024). P (MMA-co-MAA)/cellulose nanofibers composites: Effect of hydrogen bonds on molecular mobility. *Carbohydrate Polymers*, *346*, 122579.
-

- 
- [34] Fahrländer, M., Bruch, M., Menke, T., & Friedrich, C. (2001). \*Rheological behavior of PS-melts containing surface modified PMMA-particles\*. Rheologica Acta, 40(1), 1-9.
- [34] Ghaffar, S. H., & Fan, M. (2023). \*Bio-based adhesives for wood composites: A review\*. Coatings, 14(6), 774.
- [36] World Health Organization (WHO). (2010). Exposure to benzene: A major public health concern. WHO Document.
- [37] Agency for Toxic Substances and Disease Registry (ATSDR). (2007). Toxicological profile for toluene, xylene, and methyl ethyl ketone. U.S. Department of Health and Human Services.
- [38] Frihart, C. R. (2015). Wood adhesives: Chemistry and technology of their environmental impact. Green Chemistry, 17(2), 118-132.
- [39] alvez et al., 2024 - Recent Advances in Bio-Based Adhesives and Formaldehyde-Free Technologies.
- [40] Calovi et al., 2024 - Recent Advances in Bio-Based Wood Protective Systems.
- [41] Ghaffar, S. H., & Fan, M. (2024). Biobased adhesives and coatings: Environmental impact and carbon-footprint reduction. Coatings, 14(6), 60774.
-